Heliyon 10 (2024) e25869

Contents lists available at ScienceDirect

Heliyon

journal homepage: www.cell.com/heliyon

Research article

Liquid-core polymer nanocapsules prepared using flash nanoprecipitation

Sophia Taylor [1], Yuri Chung [1], Samuel Becker, Eleni Hughes [*], Xinran Zhang, Edward Van Keuren

Department of Physics and Institute for Soft Matter Synthesis and Metrology, Georgetown University, 37th & O Sts. NW, Washington DC, USA

ARTICLE INFO

Keywords:
Polymers
Nanoparticles
Nanocapsules
Flash nanoprecipitation
Nanoparticle synthesis

ABSTRACT

Hypothesis: Nanocapsules, consisting of a solid shell and a liquid core, are an interesting class of materials with numerous applications and various methods of synthesis. One common method for synthesis of nanoparticles is flash nanoprecipitation. For a multicomponent system consisting of a liquid (n-hexadecane) and solid (polystyrene), we hypothesize that nanocapsules will form from droplets created by the turbulent mixing in the nanoprecipitation process. We anticipate n-hexadecane molecules should phase-separate more rapidly from the non-solvent, thus becoming the core, while the more slowly diffusing polystyrene forms the shell. Additionally, we predict that the amount of both n-hexadecane and polystyrene used in creating these nanocapsules will influence capsule size.

Experiments: Using flash nanoprecipitation, we synthesized nanocapsules of a polystyrene shell and liquid core of n-hexadecane. We varied the concentrations of both polystyrene and n-hexadecane and characterized the resulting dispersions using dynamic light scattering and scanning electron microscopy.

Findings: Our experiments demonstrate that flash nanoprecipitation can be employed to create nanocapsules with radii ranging from 50 to 200 nm, with radii of the n-hexadecane cores between 35 and 175 nm and polystyrene shells with thickness ranging from 7 to 62 nm. We used various methods of analysis to confirm this core/shell morphology and applied a droplet model to explain the dependence of particle size on initial concentrations of n-hexadecane and polystyrene.

1. Introduction

The ability to incorporate multiple chemical species into single nanoparticles has greatly expanded their use in various applications. This is true for inorganic materials including ternary and quaternary blends such as those used as light harvesters [1], organic materials such as polymer blends and cocrystals [2], and composites such as the metal-halide perovskite compounds that are being developed for solar cells [3]. Both the kinetics and thermodynamics of the formation process are important in the resulting composition and morphology in these types of nanoparticles.

Room temperature solution-based synthesis methods for nanoparticles are beneficial for molecules that might degrade at high temperatures or dehydrate under vacuum. One such method, known by various names including micronization, solvent shifting, the

* Corresponding author.
E-mail address: eph44@georgetown.edu (E. Hughes).
[1] These two authors contributed equally to this work.

https://doi.org/10.1016/j.heliyon.2024.e25869
Received 3 October 2023; Received in revised form 20 December 2023; Accepted 5 February 2024
Available online 11 February 2024

reprecipitation method, and flash nanoprecipitation, relies on rapidly mixing a solution with a miscible nonsolvent [4]. The swift drop in solubility induces aggregation and/or self-assembly of the solute molecules, and at low concentrations, the formation of a metastable dispersion of nanoparticles with sizes on the order of 10's to 100's of nanometers. This has been used to create nanoparticles of a variety of organic materials including various chromophores [5], polymers [6], and drug formulations [7].

While similar methods have been developed in which the particle formation is thermodynamically favored [8], in flash nanoprecipitation it is heavily influenced by the kinetics of the mixing process. We recently showed that the formation of polystyrene nanoparticles can be accurately described using a droplet model, in which turbulent mixing leads to formation of nascent small droplets which then coalesce into the final particles [9].

In addition to single component nanoparticles, we have shown that this method can be used to create multicomponent materials such as nanococrystals [2,10,11]. Other groups have also developed multicomponent nanoparticles; for example Wu et al. synthesized liquid-core nanoparticles by injecting a polymer and oily liquid into a nonsolvent in a manner similar to that used in flash nanoprecipitation [12].

The encapsulation of a liquid phase into polymer micro or nanoparticles provides novel materials for a number of applications [13], including as corrosion inhibitors [14], nanoreactors [15], herbicide nanocarriers [16], and in biomedical applications such as drug delivery [17,18]. Micro- and nanoencapsulation of liquids has been demonstrated using a number of methods, including emulsification/solvent evaporation [19], in-situ polymerization [20], phase separation followed by photopolymerization, nanoprecipitation [21] and chemically induced nucleation and growth followed by surface passivation [22]. These methods generally rely on quasi-equilibrium processes such as miniemulsion or microemulsion polymerization [23].

Here we use flash nanoprecipitation to create nanocapsules with a liquid core of n-hexadecane surrounded by a polystyrene shell. We show that the formation of the core-shell morphology is consistent with our model of droplets of the injected fluid formed by the turbulent mixing from the precursors. We also show that while the fluid is retained in the shells even after drying, it can be removed by high shear, leading to the collapse of the shell. Finally, we use a novel combination of dynamic light scattering and fluorescence correlation spectroscopy to verify the core-shell structure of the nanocapsules.

2. Experimental methods

We prepared solutions of atactic polystyrene with a molecular weight of 260 kDa (Scientific Polymer Products) in tetrahydrofuran (THF) at concentrations ranging from 0.1 to 2.0 mg/mL. These are all below the overlap concentration c* (3.1 mg/mL) [24]. To create liquid-core nanoparticles, a volume of n-hexadecane was added to give volume ratios of PS:hexadecane ranging from 1:0 to 1:2. This solution was rapidly injected through an 18 gauge pipet needle (inner diameter = 0.838 mm) into distilled water with a 1:19 (solution: water) volume ratio at a rate of 1.0 mL/s using an automated syringe pump (Hamilton Microlab 500). The water was vortexed at a rate of 1000 rpm during and after the injection. The rates of injection and vortexing result in Reynold's numbers $> 10^3$, implying turbulent mixing of the THF solution and water [9]. THF was removed from the samples after mixing by slow evaporation of uncovered vials placed in a fume hood over a period of several days.

Particle sizes were measured using a custom-built dynamic light scattering (DLS) apparatus based on an ALV-5000 hardware autocorrelator (ALV GmbH). Details of the apparatus and data analysis can be found in reference [25]. A second-order cumulant analysis was used to give z-average particle sizes. These results were corroborated using a Litesizer 500 (Anton Paar USA Inc.), which was also used for measurements of the zeta potential. Atomic force microscopy (AFM) images were taken using an NTEGRA Prima AFM (NT-MDT Spectrum Instruments). Scanning electron microscopy (SEM) was carried out using a Zeiss Supra 55VP with a secondary electron detector at 0.5 kV–2 kV beam energy. Transmission electron microscopy (TEM) imaging was performed with a JEM2100 Plus (JEOL) instrument equipped with a LaB6 electron source operating at an acceleration voltage of 200 kV. Samples for AFM and SEM were prepared by several methods. Spin coating was performed using a Laurell spin coater (Model WS-650-MZ-23NPPBD) at a speed of 500 rpm for 1 min followed by 2000 rpm for an additional minute. Some samples for imaging were also drop-cast from solution. Si wafers were used as substrates and washed with acetone followed by cleaning with an air plasma prior to deposition.

For the light scattering measurements, four different sample sets were prepared for each concentration and ratio of polystyrene to hexadecane. The particle size data shown later are averages over the four sets, with the error bars showing the error of the mean.

Fluorescence correlation spectroscopy measurements were conducted using a custom-built instrument. Laser light from a 405 nm laser diode mounted on a temperature-controlled mount was spatially filtered to give a TEM00 spatial profile beam. The beam was reflected from a dichroic mirror and focused into the suspensions with a 60X water immersion objective with numerical aperture 1.2 (Olympus UPlanAPO). The emitted fluorescence passed through a long pass optical filter to remove any direct laser light and then through a 15 μm diameter pinhole placed in a plane confocal with the focused spot in the sample. Finally, the light was focused onto a single photon counting avalanche photodiode (PerkinElmer SPCM-AQR-13). The fluctuations in the fluorescence emitted from the confocal volume were analyzed with a hardware autocorrelator (ALV 5000) to yield photon count autocorrelation functions, which were fit to the standard functional form assuming 2-dimensional diffusion [26].

3. Results and discussion

3.1. Nanocapsule formation

Upon injection of the polystyrene/hexadecane solution in THF into water with a pH of 7.6, the sample immediately became turbid, indicating the formation of scatterers with sizes on the order of tens of nm or larger. The samples were stable over a period of weeks,

without phase separation or precipitation. This stability was confirmed with zeta potential measurements, which gave values ranging from −17.5 to −40.7 mV, depending on the ratio of polystyrene to hexadecane, but with no clear trends. Surface charges on polymer nanoparticles prepared using flash nanoprecipitation have been attributed to ionic end-groups, which depend on the type of initiator used in their synthesis [27].

Fig. 1 shows the particle volume calculated from the radii measured by DLS and assuming a spherical geometry, as a function of the initial concentrations of the polystyrene in THF for the 2:1 vol ratio of n-hexadecane to polystyrene [28]. These measurements were taken immediately after the flash nanoprecipitation process, so the particles are suspended in a binary solvent of 95% water, 5% THF, i.e., all samples are in an identical solvent. In single component polystyrene nanoparticles, we previously found a linear dependence of volume on the initial polymer concentration, which we explained using a droplet model [9]. This linear dependence is not observed for the polystyrene/hexadecane nanoparticles, but the addition of n-hexadecane to the polymer solution did result in larger particles, suggesting that it is being incorporated into the particles.

However, the particle sizes were larger than would be expected from only the addition of hexadecane to the particle volume. We suspected that this was due to some of the THF solvent being incorporated into the particle in order to solubilize the hexadecane. In order to check this hypothesis, we left samples uncovered for several days in order to allow THF in the solvent to evaporate, which should in turn reduce the liquid volume within the particles as the solvents inside and outside of the particles equilibrate. After letting the THF evaporate from the sample for 48 h, the volumes not only decreased substantially, but now appear to follow a linear dependence of particle volume on the volume of polymer injected into the water, similar to the trend seen in single-component polystyrene nanoparticles synthesized with this method [9]. Fig. 2 shows these data for several different ratios of hexadecane and polystyrene (Fig. S1 in the supplemental materials shows the same data plotted as radius vs. concentration) [28]. In addition to the reduction in size, the standard deviations of the data points decreased substantially. Measurements of the particle size vs. time in an uncovered sample from which the THF was evaporating are shown in Fig. S2 in the supporting information, where there is a slow decrease in the particle size over the course of about 10 h, similar to the effect seen in Figs. 1 and 2.

The THF swelling effect was more pronounced in samples with a higher ratio of polymer/hexadecane solution to water, as seen in the supporting information Figs. S3 and S4, which depict samples prepared with a 1:9 solution:water volume ratio. Similar behavior was observed: the initial dependence of particle volume on concentration was nonlinear, but after evaporation of the THF, it became linear and with the expected dependence on the concentrations of polymer and hexadecane. The size of the particles in samples that were left uncovered for a day decreased even for particles without hexadecane, suggesting that even the pure polystyrene nanoparticles are initially swollen with THF.

In the droplet model of particle formation during flash nanoprecipitation, the injected stream rapidly breaks up into regions of high polymer concentration during the turbulent mixing. The size of these droplets depends only on the mixing conditions. As the solvent and non-solvent interdiffuse, the polymer in the droplets coalesces into solid particles, with their volume equal to the total amount of material (polymer plus liquid core) that is contained within them. Hence we observe a linear relationship between the particle volume and the polystyrene concentration.

Some deviation from this model was seen when plotting the particle volumes as a function of the total concentration (polystyrene plus hexadecane), where we would expect the curves to lie on top of each other (supporting information Fig. S5). This could be due to systematic error in determining the concentration of hexadecane, which is typically added in amounts on the order of tens of μL. It may also be the case that the different amounts of added hexadecane affect the propensity of the droplets to coalesce before the polymer reaches the glass transition, since the hexadecane may partially plasticize the polystyrene. Nevertheless, the linearity of the nanocapsule size with the volume of polystyrene plus hexadecane is clearly evident in all samples.

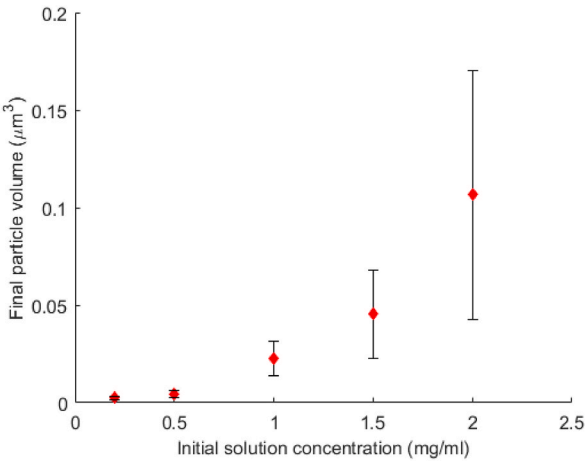

Fig. 1. Particle volume vs. initial polymer concentration for particles with a 2:1 ratio of hexadecane to polystyrene measured taken immediately after flash nanoprecipitation. Volumes were calculated using the particle radius measured using DLS, assuming spherical particles.

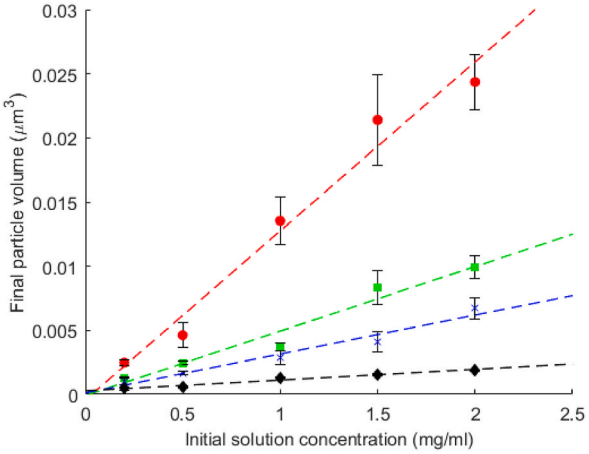

Fig. 2. Particle volumes vs. concentration of polystyrene after evaporation of THF for 48 h for all four ratios of n-hexadecane to polystyrene (red circles 2:1, green squares 1:1, blue crosses 0.5:1, black diamonds 0:1). The dotted lines are linear fits to the data.

3.2. Core-shell morphology

SEM images of dried particles suggest that the particles have a core-shell structure. Dispersions of the particles were spin-coated onto a silicon substrate. Fig. 3 shows images of particles with different volumes of added hexadecane (these volume ratios of polystyrene to hexadecane were: no hexadecane, 2:1, 1:1, and 1:2). These were consistent with the DLS results, showing larger particles but thinner shells with increasing amounts of hexadecane. The images display a much more pronounced shell structure compared to those

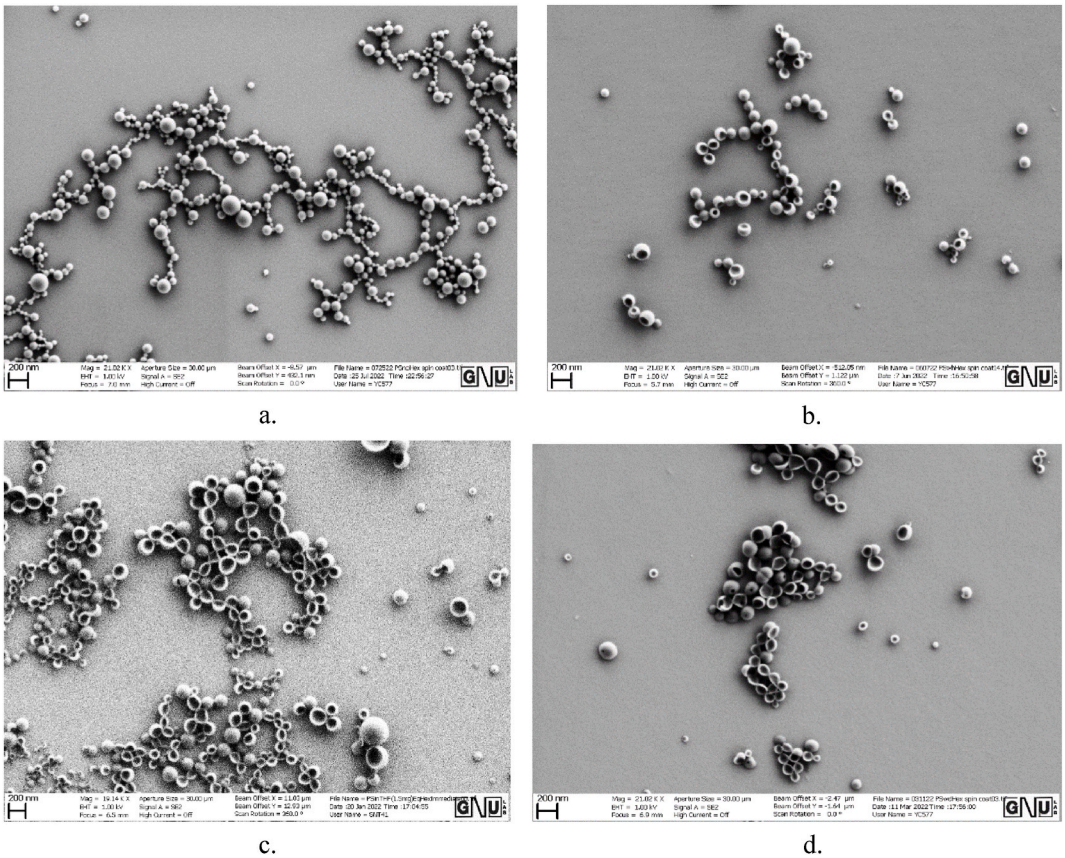

Fig. 3. SEM images of particles. From the top, the particles contained ratios of n-hexadecane to polystyrene if (a) 0:1, (b) 0.5:1, (c) 1:1, and (d) 2:1. All samples had an initial polystyrene concentration of 1.5 mg/mL.

observed by Wu et al. [12], possibly due to the higher glass transition temperature of polystyrene (104 °C) compared to that of shellac, the polymer used in their report (42 °C).

These images are corroborated by images of the same samples using AFM and TEM (supporting information Figs. S6 and S7). We also imaged dispersions that were prepared by drop-casting using SEM (see supporting information Fig. S8). Primarily spherical particles were observed in both cases, often with pores in the polymer shell. This suggests that the high-speed during spin coating leads to the collapsed shell structures, with the entrapped hexadecane removed by the large shear experienced by the particle during spin coating.

3.3. Fluorescence correlation spectroscopy

We found further evidence for the liquid core/polymer shell morphology using fluorescence correlation spectroscopy (FCS), a method in which the diffusion coefficient of molecules or small particles can be measured [26]. This method is based on fluctuations in the fluorescence from dilute fluorophores in a very small sampling volume. We prepared a sample in which the fluorophore perylene was added to the polystyrene and hexadecane solution. This dye partitions roughly equally into hexadecane and the polymer (log P = −0.23), as shown in Fig. S9 in the supporting information, so we expect contributions to the fluorescence signal from dye in both compartments.

FCS measurements of these nanocapsules yielded a narrow range of diffusion coefficients. Fig. S10 depicts a typical autocorrelation function obtained from the dye-doped nanocapsules. Moreover, these matched the corresponding diffusion coefficients measured using dynamic light scattering. DLS characterizes the diffusion coefficient of the physical particles, while in FCS the diffusion coefficient of the object that is emitting the fluorescence is measured, in this case, the perylene dissolved in hexadecane. The fact that these diffusion coefficients showed an excellent match, as shown in Table 1, implies that the hexadecane is contained in the particles while they are suspended in the aqueous phase, i.e., both polymer shell and liquid core are diffusing together.

We calculate the relative thicknesses of the core and shell for a given volume ratio as

$$r_c = r_p \sqrt[3]{\frac{R}{1+R}}$$

$$r_s = r_p - r_c$$

where r_p, r_c and r_s are the radii of the particle, core and shell, respectively, and R is the volume ratio of the liquid to polymer. Table 1 also lists the calculated shell radii for the 1:1 vol ratio nanocapsule. While a precise measurement of the shell thickness cannot be done from the SEM images, the values in the table seem to roughly coincide with the images in Fig. 3c.

3.4. Droplet model

Our results can be understood within the context of the droplet model that we developed for single polymer component nanoparticles prepared by flash nanoprecipitation. According to this model, the injected solution rapidly breaks into droplets due to the turbulent mixing [9,29]. The size of the droplets is determined by the fluid dynamics: the mixing conditions and fluid properties. While these droplets form, the solvent and non-solvent interdiffuse, leading to the hydrophobic components that are initially dissolved in the solution, in this case, polystyrene and n-hexadecane, to become highly supersaturated. As depicted schematically in Fig. 4, the free energy gradient at the droplet surface results in diffusion of the hydrophobic components away from the interface. The faster rate of diffusion of the hexadecane ensures that it reaches the particle center first, while the slower diffusing polystyrene chains will be more concentrated at the surface. As in single component polystyrene nanoparticles formed with this method, it will reach its glass transition at some point, locking in its shell structure.

In this model, both the diffusivity and hydrophobicity of the molecules relative to that of the polymer dictate whether the resulting particles have a core-shell morphology. For example, for a polymer and small molecule with equal hydrophobicities, the slower diffusion of the polymer will lead to the small molecule phase separating into the core of the droplet while the polymer diffuses toward the core more slowly. If the polymer reaches a glass transition, this core-shell structure will be fixed into place. This may occur even for mildly hydrophobic molecules, which would enable the entrapment of small molecules with moderate water solubility. However, this dependence is likely to be complex, since the concentration profiles of all four components (two solvents, polymer and liquid core) are

Table 1
Diffusion coefficients measured by DLS and FCS for perylene-doped nanocapsules prepared at different concentrations. All samples had a 1:1 vol ratio of polystyrene to hexadecane.

Sample concentration (mg/mL)	Diffusion coefficient from DLS ($\mu m^2/s$)	Diffusion coefficient from FCS ($\mu m^2/s$)	Particle radius calculated from DLS diffusion coefficient (nm)	Calculated shell thickness (nm)
2.0	1.31	1.03	139	29.2
1.5	1.56	1.73	116	24.3
1.0	1.93	1.85	94.3	19.8
0.5	2.16	2.36	84.2	17.7
0.2	2.54	2.57	71.6	15.0

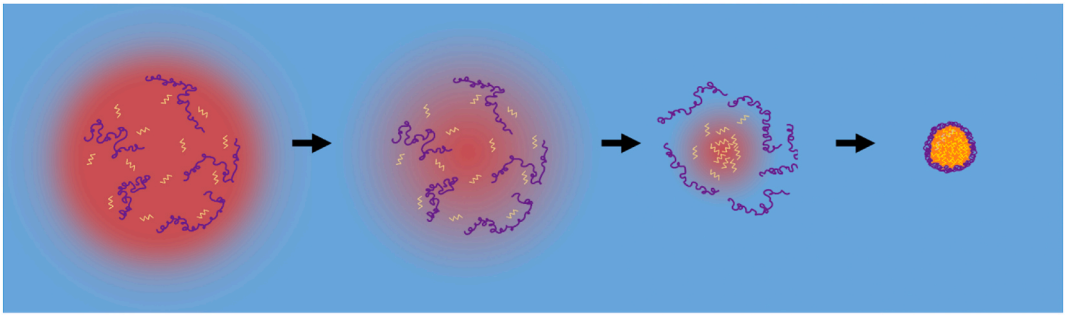

Fig. 4. Schematic diagram of the core-shell formation. The red-tinted area represents the good solvent (THF) while the blue background is the non-solvent (water). The n-hexadecane is represented by the yellow lines and the polystyrene by the purple lines.

changing simultaneously.

The initial droplet size depends primarily on the mixing conditions, and as such will be comparable for all samples regardless of polymer or n-hexadecane concentration. The final particle sizes then depend on how much material is contained in the droplets, i.e., we expect the observed linear relation between the initial concentration of polymer and n-hexadecane and the final particle volume.

4. Conclusion

The method of flash nanoprecipitation has been shown to be a simple and effective method for creating a wide variety of single [1–3] and multicomponent nanoparticles [4,5]. Here we have shown that this method can also be used to create liquid-core/polymer-shell nanocapsules. Using dynamic light scattering, we were able to demonstrate that liquid n-hexadecane can be encapsulated within polystyrene nanoparticles, while electron microscopy data was used to infer a core/shell morphology. We further corroborated this with fluorescence correlation spectroscopy measurements of a dye partially dissolved in the liquid phase, which gave nearly identical values of diffusivity as those determined from light scattering. These particles had radii ranging from 60 nm to 160 nm and shell thicknesses ranging from 10 to 35 nm. Compared to other methods for synthesizing nano- and microcapsules [8,12–23], flash nanoprecipitation greatly extends the range of materials for both the core and shell and provides some control over the particle size. We have also developed a model that provides a more consistent picture of the formation than previous reports [12]. We hypothesize that the core-shell structure arises from the different diffusivities of the two components as well as their differing interactions with the solvent and non-solvent. This model describes the results of our experiments well and is consistent with results of earlier investigations [9]. It also provides a useful framework for creating a wide range of liquid core nanocapsules, with applications in numerous areas including food packaging, medical diagnostics and drug delivery [13].

Data availability

The raw data required to reproduce these findings are available to download from https://doi.org/10.17632/rtpng3nv2y.1. The processed data required to reproduce these findings are available to download from https://doi.org/10.17632/rtpng3nv2y.1.

CRediT authorship contribution statement

Sophie Taylor: Writing – original draft, Formal analysis, Data curation, Conceptualization. **Yuri Chung:** Formal analysis, Data curation. **Samuel Becker:** Formal analysis, Data curation. **Eleni Hughes:** Writing – review & editing, Methodology, Investigation, Conceptualization. **Xinran Zhang:** Supervision, Methodology, Investigation. **Edward Van Keuren:** Supervision, Methodology, Conceptualization.

Declaration of competing Interest

The authors declare that they have no known competing financial interests or personal relationships that could have appeared to influence the work reported in this paper.

Acknowledgements

TEM imaging was carried out in the Chemistry Research Facilities at American University. Support for ST and YC came from a pilot grant from Georgetown University and from the NASA DC space grant consortium. ST was also supported by the Hichwa Family Summer Undergraduate Fellowship.

Appendix A. Supplementary data

Supplementary data to this article can be found online at https://doi.org/10.1016/j.heliyon.2024.e25869.

References

[1] C.S. Bagade, V.B. Ghanwat, E. Van Keuren, P.N. Bhosale, A robust and self-assembled route to synthesis of CdZn(Se1-xTex)(2) photoanodes as light harvesters for photoelectrochemical solar cells, J. Mater. Sci. Mater. Electron. 29 (2018) 11763–11773.
[2] E. Van Keuren, M. Nishida, Synthesis of nanocomposite materials using the reprecipitation method, CMC-Comput. Mater. Con. 409 (2010) 61–77.
[3] M.K. Assadi, S. Bakhoda, R. Saidur, H. Hanaei, Recent progress in perovskite solar cells, Renew. Sustain. Energy Rev. 81 (2018) 2812–2822.
[4] D. Horn, Preparation and characterization of microdisperse bioavailable carotenoid hydrosols, Angew. Makromol. Chem. 166 (1989) 139–153.
[5] H. Kasai, H.S. Nalwa, H. Oikawa, S. Okada, H. Matsuda, N. Minami, A. Kakuta, K. Ono, A. Mukoh, H. Nakanishi, Novel preparation method of organic microcrystals, Jpn. J. Appl. Phys. 31 (1992) L1132–L1134. Part 2.
[6] C. Zhang, V.J. Pansare, R.K. Prud'homme, R.D. Priestley, Flash nanoprecipitation of polystyrene nanoparticles, Soft Matter 8 (2012) 86–93.
[7] S.M. D'Addio, R.K. Prud'homme, Controlling drug nanoparticle formation by rapid precipitation, Adv. Drug Deliv. Rev. 63 (2011) 417–426.
[8] H. Fessi, F.D. Puisieux, Nanocapsule Formation by interfacial polymer deposition following solvent displacement, Int. J. Pharm. 55 (1989) R1–R4.
[9] C. Zhao, S. Melis, E.P. Hughes, T. Li, X. Zhang, P.D. Olmsted, E. Van Keuren, Particle Formation mechanisms in the nanoprecipitation of polystyrene, Langmuir 36 (2020) 13210–13217.
[10] T. Li, S. Melis, C. Bagade, A. Khatib, R. Kosarzycki, G. Maglieri, X. Zhang, E. Van Keuren, Mechanisms of nucleation and growth in the formation of charge transfer nanocrystals, J. Nano Res. 21 (2019) 147.
[11] E. Van Keuren, S. Melis, In Charge transfer nanocrystals for optical and electronic applications, in: L.R.P. Kassab, S.J.L. Ribiero, R. Rangel-Rojo (Eds.), Nanocomposites for Photonic and Electronic Applications, Elsevier, 2020, pp. 139–165.
[12] B.H. Wu, C.J. Yang, B. Li, L. Feng, M. Hai, C.X. Zhao, D. Chen, K. Liu, D.A. Weitz, Active encapsulation in biocompatible nanocapsules, Small 16 (2020) 2002716.
[13] H.N. Yow, A.F. Routh, Formation of liquid core–polymer shell microcapsules, Soft Matter 2 (2006) 940–949.
[14] V.A. Golovin, S.A. Tyurina, Microencapsulation of corrosion inhibitors and active additives for anticorrosive protective polymer coatings, International Journal of Corrosion and Scale Inhibition 8 (2019) 179–198.
[15] D. Crespy, M. Stark, C. Hoffmann-Richter, U. Ziener, K. Landfester, Polymeric nanoreactors for hydrophilic reagents synthesized by interfacial polycondensation on miniemulsion droplets, Macromolecules 40 (2007) 3122–3135.
[16] M. Diyanat, H. Saeidian, S. Baziar, Z. Mirjafary, Preparation and characterization of polycaprolactone nanocapsules containing pretilachlor as a herbicide nanocarrier, Environ. Sci. Pollut. Res. 26 (2019) 21579–21588.
[17] C. Tomaro-Duchesneau, S. Saha, M. Malhotra, I. Kahouli, S. Prakash, Microencapsulation for the therapeutic delivery of drugs, live mammalian and bacterial cells, and other biopharmaceutics: current status and future directions, Journal of Pharmaceutics 2013 (2012) 103527.
[18] C.E. Mora-Huertas, H. Fessi, A. Elaissari, Polymer-based nanocapsules for drug delivery, Int. J. Pharm. 385 (2010) 113–142.
[19] A. Loxley, B. Vincent, Preparation of poly(methylmethacrylate) microcapsules with liquid cores, J. Colloid Interface Sci. 208 (1998) 49–62.
[20] S.R. White, N.R. Sottos, P.H. Geubelle, J.S. Moore, M.R. Kessler, S.R. Sriram, E.N. Brown, S. Viswanathan, Autonomic healing of polymer composites, Nature 409 (2001) 794–797.
[21] J.D. Echeverri, S. Guerrero-Escalante, C.H. Salamanca, Relationship between the process variables and physicochemical features of liquid-core nanocapsules produced via nanoprecipitation, Biointerface Research in Applied Chemistry 9 (2019) 4037–4043.
[22] R. Wang, F. Han, B. Chen, L. Liu, S. Wang, H. Zhang, Y. Han, H. Chen, Liquid nanoparticles: manipulating the nucleation and growth of nanoscale droplets, Angew. Chem. Int. Ed. 60 (2021) 3047–3054.
[23] J. Jang, K. Lee, Facile fabrication of hollow polystyrene nanocapsules by microemulsion polymerization, Chem. Commun. 2 (2002) 1098–1099.
[24] E.D. Von Meerwall, E.J. Amis, J.D. Ferry, Self-diffusion in solutions of polystyrene in tetrahydrofuran - comparison of concentration dependences of the diffusion-coefficients of polymer, solvent, and a ternary probe component, Macromolecules 18 (1985) 260–266.
[25] E. Van Keuren, A. Bone, C. Ma, Phthalocyanine nanoparticle formation in supersaturated solutions, Langmuir 24 (2008) 6079–6084.
[26] R. Rigler, U. Mets, J. Widengren, P. Kask, Fluorescence correlation spectroscopy with high count rate and low-background - analysis of translational diffusion, Eur. Biophys. J. Biophys. Lett. 22 (1993) 169–175.
[27] K. Roger, M. Eissa, A. Elaissari, B. Cabane, Surface charge of polymer particles in water: the role of ionic end- groups, Langmuir 29 (2013) 11244–11250.
([28]S. Taylor, Y. Chung, S. Becker, E. Hughes, X. Zhang, E. Van Keuren, "Liquid-core Polymer Nanocapsules Prepared Using Flash Nanoprecipitation", vol. 1, Mendeley Data, 2023.
[29] D. Franke, W. Gosele, Modeling precipitation with a hydrodynamic approach, Chem. Ing. Tech. 71 (1999) 1245–1252.